Phytopathology® • 2023 • 113:2127-2133 • https://doi.org/10.1094/PHYTO-09-22-0357-SA

Pathogen Spotlight

Genetics and Genomics of Resistance

Exploring the Relationship Between Pattern-Triggered Immunity and Quantitative Resistance to *Xanthomonas vasicola* pv. *vasculorum* in Maize

Alexander Mullens,[1] Alexander E. Lipka,[1] Peter Balint-Kurti,[2,3] and Tiffany Jamann[1,†]

[1] Department of Crop Sciences, University of Illinois Urbana-Champaign, Urbana, IL 61801
[2] Department of Entomology and Plant Pathology, North Carolina State University, Box 7616 Raleigh, NC 27695
[3] Plant Science Research Unit, U.S. Department of Agriculture-Agricultural Research Service, Raleigh, NC 27695
Accepted for publication 21 February 2023.

Abstract

Bacterial leaf streak (BLS) of maize is an emerging foliar disease of maize in the Americas. It is caused by the gram-negative nonvascular bacterium *Xanthomonas vasicola* pv. *vasculorum*. There are no chemical controls available for BLS, and thus, host resistance is crucial for managing *X. vasicola* pv. *vasculorum*. The objective of this study was to examine the genetic determinants of resistance to *X. vasicola* pv. *vasculorum* in maize, as well as the relationship between other defense-related traits and BLS resistance. Specifically, we examined the correlations among BLS severity, severity for three fungal diseases, flg-22 response, hypersensitive response, and auricle color. We conducted quantitative trait locus (QTL) mapping for *X. vasicola* pv. *vasculorum* resistance using the maize recombinant inbred line population Z003 (B73 × CML228). We detected three QTLs for BLS resistance. In addition to the disease resistance QTL, we detected a single QTL for auricle color. We observed significant, yet weak, correlations among BLS severity, levels of pattern-triggered immunity response and leaf flecking. These results will be useful for understanding resistance to *X. vasicola* pv. *vasculorum* and mitigating the impact of BLS on maize yields.

Keywords: bacterial leaf streak, maize, pattern-triggered immunity, quantitative disease resistance, *Xanthomonas*

Bacterial leaf streak (BLS) of maize is a new and emerging disease, caused by the gram-negative bacterium *Xanthomonas vasicola* pv. *vasculorum* (Lang et al. 2017; Ortiz-Castro et al. 2020), which is threatening to reduce maize yields in the Americas. *X. vasicola* pv. *vasculorum* was first identified in 2014 in the United States in Nebraska and has subsequently been confirmed throughout many of the corn-growing regions of the Midwest (Damicone et al. 2018; Jamann et al. 2019; Korus et al. 2017). Prior to its discovery in the United States, it had not been observed outside South Africa, where it was first described in 1949 (Dyer 1949). Outbreaks in Argentina and Brazil have also been reported (Leite et al. 2019; Plazas et al. 2018).

In maize, *X. vasicola* pv. *vasculorum* behaves as a nonvascular foliar pathogen that colonizes the intercellular space of the mesophyll (Ortiz-Castro 2019; Ortiz-Castro et al. 2020). The visual symptoms include long brown with yellow water-soaked lesions that are constricted to the interveinal spaces (Coutingo and Wallis 1991). Lesions can cover 40 to 50% of the leaf area (Korus et al. 2017). The high percentage of foliar lesion coverage suggests that there is a potential for yield loss due to decreased photosynthetic area of the leaves. However, the true potential for yield loss has not been determined. A diverse array of plant species are hosts for *X. vasicola* pv. *vasculorum* (Hartman et al. 2020a; Lang et al. 2017). In Africa and South America, *X. vasicola* pv. *vasculorum* is also a pathogen of sugarcane, where it behaves primarily as a xylem-colonizing vascular pathogen causing sugarcane gumming disease (Lang et al. 2017; Ortiz-Castro et al. 2020).

It has been hypothesized that the relatively sudden emergence and spread of *X. vasicola* pv. *vasculorum* in the Americas is in part due to the evolution of a novel, more virulent lineage of the pathogen. There was genetic exchange between *X. vasicola* pv. *vasculorum* and *X. vasicola* pv. *holcicola*, a pathogen that causes minor disease on maize and sorghum (Perez-Quintero et al. 2020). The *X. vasicola* pv. *vasculorum* isolates from North and South America that have been sequenced carry a gene cluster that appears to have been derived from *X. vasicola* pv. *holcicola*, but most isolates of *X. vasicola* pv. *vasculorum* from South Africa lack these sequences (Perez-Quintero et al. 2020). It is hypothesized that this gene cluster might be involved in adaptation of the American population. Phylogenetic analyses of African, South American, and North American isolates indicate that there were likely two introduction events from South Africa into North and South America, with the first in the late 1990s and a second event between 2001 and 2010 (Perez-Quintero et al. 2020).

Management strategies for BLS include crop rotation with nonhost crops, removal of crop residue through tillage practices, and planting hybrids with genetic sources of resistance (Barak et al. 2001; Gent et al. 2005; Hartman et al. 2020b; Longhi et al. 2022; Ortiz-Castro et al. 2020). There are no effective chemical controls without phytotoxicity that can be used by growers to control the disease (Duin et al. 2022; Longhi et al. 2022). Due to the relatively recent emergence of *X. vasicola* pv. *vasculorum*, not much is known about the genetic determinants of resistance to this pathogen. Some commercial hybrids and diverse inbred lines have been screened for resistance to BLS (Qiu et al. 2020b; Robaina et al. 2020). Only one study so far has reported the mapping of BLS resistance quantitative trait loci (QTLs). Qiu et al. (2020b) mapped several QTLs associated with BLS resistance using three biparental populations. Some of the QTLs colocalized with resistance to other bacterial and fungal diseases (Qiu et al. 2020a).

Plants lack adaptive immune systems and thus are dependent on innate, genetically controlled immune responses and preformed

†Corresponding author: T. Jamann; tjamann@illinois.edu

Funding: Support was provided by the National Science Foundation (2154872).

e-Xtra: Supplementary material is available online.

The author(s) declare no conflict of interest.

defenses. Nonspecific plant immune responses are triggered when pattern recognition receptors on the surface of cells bind to and recognize molecules that contain pathogen-associated molecular patterns (PAMPs). The resulting immune response is characterized by the production of reactive oxygen species (ROS), callose deposition, stomatal closure, and growth retardation (Boller and Felix 2009; Jones and Dangl 2006; Lloyd et al. 2014). The strength of pattern-triggered immunity (PTI) responses has been shown to vary across different lines in several plant species, including Arabidopsis, rapeseed, tomato, sorghum, and maize (Bhattarai et al. 2016; Kimball et al. 2019; Lloyd 2014; Samira et al. 2020; Vetter et al. 2012; Wang et al. 2021; Zhang et al. 2017). In Arabidopsis and tomato, the strength of the PTI response to flagellin, a common PAMP, and disease severity were negatively correlated, where Arabidopsis and tomato lines with stronger PTI responses were more resistant to *Pseudomonas syringae* pv. *tomato* and *Xanthomonas perforans*, respectively (Bhattarai et al. 2016; Vetter et al. 2012).

A recombinant inbred line (RIL) population derived from a B73 × CML228 cross was used to map the genetic determinants of variation in the strength of the PTI response elicited by flg22 and chitooctaose (C8), a fungal PAMP (Wang et al. 2021; Zhang et al. 2017). Flg22 is an epitope derived from bacterial flagellin, which is present in the flagellum of *X. vasicola* pv. *vasculorum* and other motile bacteria. No strong relationships among PTI response and disease severity of three fungal diseases in maize were found. However, this population has not been evaluated for resistance to any bacterial diseases (Wang et al. 2021; Zhang et al. 2017). Additionally, the population has been evaluated for the strength of the hypersensitive defense response, rapid cell death at the site of pathogen penetration that is triggered by the recognition of specific pathogen-derived effector proteins that are introduced into the plant cell as part of the pathogenesis process (Balint-Kurti 2019; Coll et al. 2011).

The importance of PTI and other defense-related traits in plant quantitative disease resistance has largely not been elucidated. Here, we tested the hypotheses that (i) the B73 × CML228 RIL population has novel loci conferring resistance to BLS, (ii) the genetic architecture controlling resistance and PTI are related, and (iii) there is a relationship between BLS resistance and other traits related to defense.

Materials and Methods

Experimental design

An RIL population (referred to as population Z003) derived from a B73 × CML228 cross ($n = 163$) was challenged with *X. vasicola* pv. *vasculorum* and evaluated for disease severity. Three replications of the population were planted in a greenhouse at the Plant Care Facility at the University of Illinois Urbana-Champaign in 2020. The room was maintained at 22.5 to 24.5°C during the day and 16.5 to 18.5°C at night. Supplemental lighting was provided for 12 h each day. Seeds were planted in general-purpose potting mix (1 soil/1 peat/1 perlite) in a 3.77-liter (1-gallon) pot. Three seeds were planted per pot, and seedlings were thinned to one plant per pot. Each pot was amended with 8 g of Osmocote (13–13–13 N–P–K). An augmented design with six blocks and five check lines (B73, Ki3, CML333, Oh7B, and CML228) per block was used. Due to limited space, only one replication could be planted and evaluated at a time.

Inoculation and disease evaluation

The *X. vasicola* pv. *vasculorum* strain 16Xvv001 that was used for inoculations originated from diseased leaf material collected in DeKalb County, Illinois, in 2016 (Jamann et al. 2019). The bacteria were grown from glycerol stocks for 2 to 3 days at room temperature, approximately 22°C, on nutrient agar Petri plates. The plates were then flooded with sterile deionized water to create a concentrated bacterial solution. The concentrated solution was diluted with sterile deionized water to an optical density at 600 nm of 0.02 (approximately 1,000,000 CFU/ml). The fourth leaves of V4-stage plants were inoculated via infiltration with a needleless syringe on both sides of the midrib midway between tip and base of the leaf (Lang et al. 2017; Qiu et al. 2020b; Schaad et al. 1996) (Fig. 1). The lesion length and leaf length were recorded in centimeters 9 days postinoculation. Both lesions per leaf were measured.

Data were collected on the third replication for auricle color (red or white) (Fig. 1). The data for color of the fourth leaf auricle were collected as a binary phenotype 9 days postinoculation. Lines with red auricles were scored as 1, and those with white auricles were scored as 0.

Phenotypic data analysis

We collected data on 163 lines (selected based on availability) grown in three replications for two different phenotypes: leaf length and lesion length. Percent lesion length (lesion length/leaf length × 100) was calculated. Lesion length was used for mapping. The residuals after fitting linear models for leaf length, lesion length, and percent lesion length were not normally distributed, so we transformed the data using the one-parameter Box–Cox transformation function in the "MASS" package in R (R Core Team 2021; Venables and Ripley 2002). The power parameter λ value of −0.4 for lesion length, −0.2 for percent lesion length, and 1.3 for leaf length were applied to their respective data sets to calculate the transformed data. The residuals of the transformed data that had been fitted to a linear model more closely resembled a normal distribution. All subsequent analyses were performed using the transformed data.

Models were run using the "lm" function from R (version 4.0.2) (R Core Team 2021). The following linear mixed model was run:

$$Y_{ijk} = \mu + G_i + R_k + B_{j(k)} + \varepsilon_{ijk}$$

with factors defined as follows: Y_{ijk} represents the measured area under the disease progress curve value from the genotype i in block j in replicate k; μ represents the grand mean; G_i represents the fixed effect of genotype i; R_k represents the fixed effect of replication k; $B_{j(k)}$ represents the fixed effect of block j nested in replication k; and ε_{ijk} represents the error associated with Y_{ijk}. For each line, a best linear unbiased estimate (BLUE) was extracted from the final models. Shapiro-Wilk tests for normality were conducted on the BLUEs in R using the "shapiro.test" function. To calculate heritability, a model was fitted using the "lmer" function from the lme4 package in R (version 4.0.2) (Bates et al. 2015; R Core Team 2021), with genotype and block nested within replication as random terms. BLUEs are included in Supplementary File S1. The variance components were then used to calculate the broad-sense heritability on a line mean basis using the following equation:

$$h^2 = \frac{\sigma_G^2}{\sigma_G^2 + \left(\frac{\sigma_e^2}{n}\right)}$$

where σ_G^2 is the genotypic variance, σ_e^2 is the error variance, and n is the harmonic mean of the number of independent measurements (replicates) taken for a particular genotype.

To assess the relationship among traits, Pearson correlations were calculated for comparisons among continuous traits. Comparisons between auricle color and the continuous traits were conducted using a biserial correlation. Both calculations were accomplished using the "cor" function in R (version 4.0.2). The "cor.mtest" and "corrplot" functions in the "corrplot" package (Wei et al. 2017) were used to determine the significance of the correlations and plot the results. For leaf length, lesion length, and percent lesion length, the BLUEs were used to calculate the correlations. We included data from previous publications for the traits listed in Table 1. The PTI response trait that we included from Zhang et al. (2017) in the correlations was flg22-induced root growth inhibition

(RL.CK.flg22). This trait was a measure of the reduction in root length of seedlings treated with the PAMP flg22 as compared with mock-treated seedlings.

QTL mapping

We used the publicly available genotypic dataset of 7,386 single-nucleotide polymorphism markers (the 0.2 cM resolution linkage map) and the corresponding consensus genetic map (Ogut et al. 2015). Briefly, the markers were generated using genotyping-by-sequencing and imputed on a 0.2-cM interval, and then a consensus genetic map was calculated for the nested association mapping population including Z003 (Ogut et al. 2015). A total of 157 individuals from the Z003 population were included in the analysis. The BLUEs for lesion length and the binary data for auricle color were used for mapping. To facilitate the comparison of mapping results across traits, we re-mapped QTLs using our parameters for flg22-induced ROS production (Zhang et al. 2017) and leaf flecking (Olukolu et al. 2016) using previously calculated best linear unbiased predictors. The "qtl" package in R (version 4.0.2) was used to conduct the mapping (Broman et al. 2003). We used the "maximum likelihood" interval mapping method to identify QTLs, using a step size of 1 and 0.01 error probability. Logarithm of odds (LOD) significance thresholds representing an experiment-wise error rate of 0.05 were determined by performing 1,000 permutations using the "scanone" function in the R package "qtl" via the Haley-Knott regression method. In addition, a two-dimensional genome scan was done using a two-QTL model with the "scantwo" function in the R package "qtl" to identify epistatic and additional additive QTLs. The "refineqtl" function was used to identify the QTL positions with maximum likelihood for a fixed QTL model by iteratively scanning the positions for QTLs in the context of a multiple-QTL model based on the positions given by scanone and scantwo. The "bayesint" function in R package "qtl" was used with default settings to calculate the interval estimate of the QTL location. Intervals were expanded to the nearest flanking markers. The "fitqtl" function in the R package "qtl" was used to calculate the percentage variance explained by QTL and estimate QTL effect sizes.

TABLE 1. Summary of traits examined in this study and data sources

Description	Abbreviation	Source
Southern corn leaf blight	SLB	Kump et al. 2011
Northern corn leaf blight	NLB	Poland et al. 2011
Leaf flecking	–	Olukolu et al. 2016
Gray leaf spot	GLS	Benson et al. 2015
flg22-induced production of reactive oxygen species	–	Zhang et al. 2017
Lesion severity of auto active R gene	LES	Olukolu et al. 2014
flg22 root growth retardation	–	Wang et al. 2021

Results

Germplasm characterization

The two phenotypic measures of BLS severity recorded were lesion length and percent lesion length, which is the percentage of the leaf length that the lesion covers. Because the correlation between these traits was extremely high (P = 1.3e-96, r = 0.97), here, we only report analyses using the lesion length data, as the heritability was slightly higher, and the QTLs had higher LOD scores for this trait. Leaf length had a significant but very weak positive correlation with lesion length (P = 0.016, r = 0.19), and the QTLs for these traits did not colocalize (see below), indicating that the traits are largely independent.

Lesion length BLUEs were normally distributed (Fig. 2). Lesion length exhibited transgressive segregation. Phenotypic data were analyzed using linear models (Table 2). The genotype term in the lesion length model was highly significant. Lesion length had a broad-sense line mean heritability of 0.67. Preliminary screenings conducted by Qiu et al. (2020b) using similar methods showed that CML228 and B73 had similar levels of susceptibility to BLS and were both moderately resistant compared with other lines. However, this population was selected because the parents showed a large difference in PTI responses, and the population had been used for mapping several other PTI-related traits and diseases previously (Wang et al. 2021; Zhang et al. 2017).

During plant growth, we observed that auricle color was segregating within the population. Leaf auricles are triangular-shaped

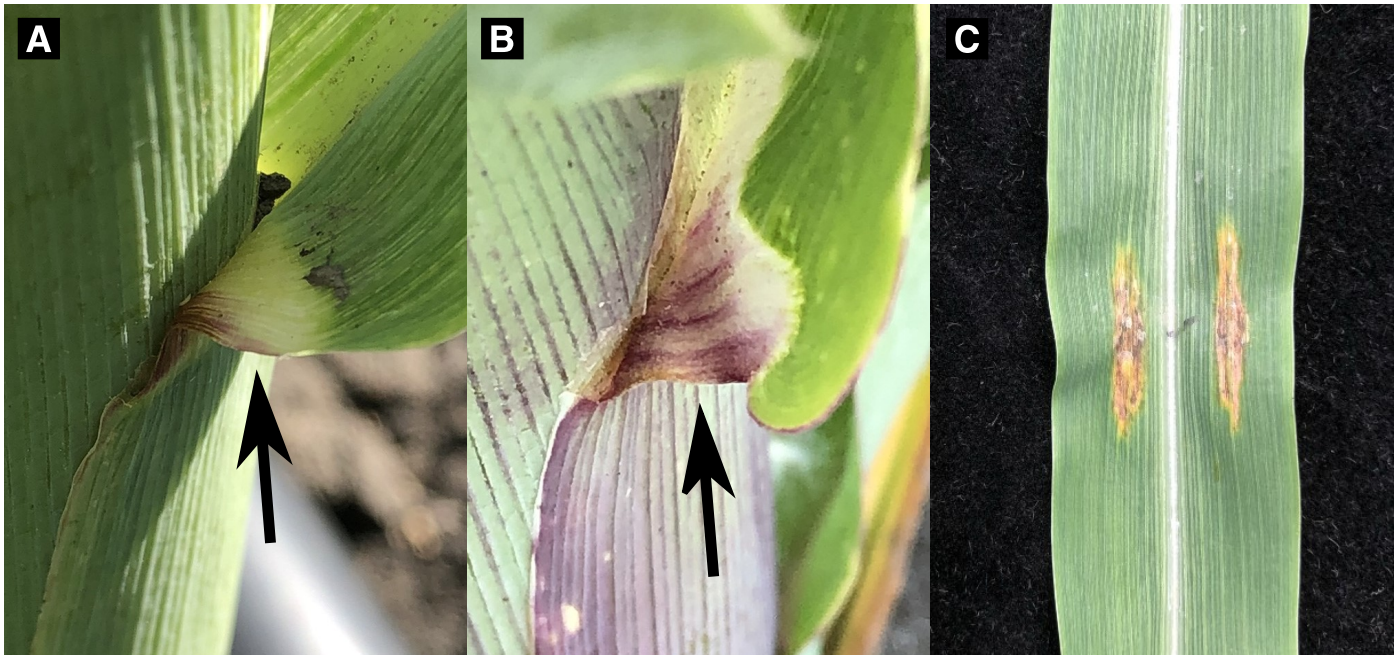

Fig. 1. Images of phenotypes examined in this study. **A,** B73 auricle; **B,** CML228 auricle; and **C,** inoculation site of a V4 stage B73 leaf infiltrated with *Xanthomonas vasicola* pv. *vasculorum*. Photo was taken at 9 days postinoculation.

portions of leaf tissue in the collar area of the leaf (base of the leaf) (Freeling and Lane 1994). We observed that CML228 had red auricles, whereas B73 had white auricles (Fig. 1). Some plants had darker auricles than either parent, suggesting that transgressive segregation may occur for this trait.

Identification of regions associated with BLS resistance and other traits

We identified significant markers using both the "scanone" and the "scantwo" functions and then tested those markers using the "fitqtl" function. We report three QTLs for lesion length. The largest effect QTL for lesion length was located in chromosomal bin 5.03, encompassing over 135 Mb and accounting for 10.3% of the total variation (Table 3), with resistance conferred by the CML228 allele (Table 3). The QTL interval was relatively large (Table 3), which might be due to multiple causative genes underlying the QTLs. There are multiple peaks in the LOD scores, but we were not able to resolve the peaks into separate QTL (Fig. 3). Two additional QTLs for lesion length were detected on chromosomes 2 and 7, with resistance conferred respectively by the CML228 allele and the B73 allele (Table 3). A QTL associated with auricle color in the fourth leaf was mapped on chromosome 6, with the CML228 allele conferring decreased auricle reddening.

Relationship among BLS resistance and other defense-related traits

We hypothesized that BLS resistance might be influenced by other traits related to defense. This population was previously assessed for several diseases and disease-related traits (Table 1) (Benson et al. 2015; Kump et al. 2011; Olukolu et al. 2016; Wang et al. 2021), and we examined the correlations among those traits and the data we collected. Although significant correlations were found among some of these traits, the correlations were relatively weak (Fig. 4). Lesion length had a weak significant negative correlation with PTI response as measured by flg22-induced root growth inhibition (RL.CK.flg22; $P = 0.049$, $r = -0.16$), where lines with more root length inhibition (stronger PTI response) had smaller lesions (less severe BLS). We examined the relationship among BLS and two hypersensitive response-related traits including the lesion severity caused by an autoactive R gene and leaf flecking (Olukolu et al. 2014). Both traits are related to the strength of the hypersensitive response. We found a weak relationship with lesion severity due to the autoactive R gene and no relationship with leaf flecking (Fig. 4).

There are hypothesized to be common mechanisms of resistance to fungal and bacterial pathogens (Wiesner-Hanks and Nelson 2016). Previous work has shown that there are regions of the genome that confer resistance to BLS, as well as one or more fungal diseases

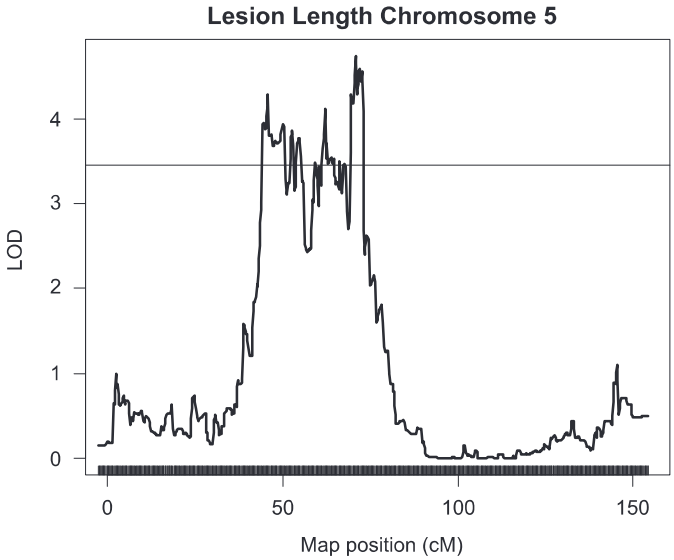

Fig. 3. Plot of chromosome 5 logarithm of odds (LOD) scores for lesion length. The line indicates the LOD significance threshold representing an experiment-wise error rate of 0.05, as determined by performing 1,000 permutations.

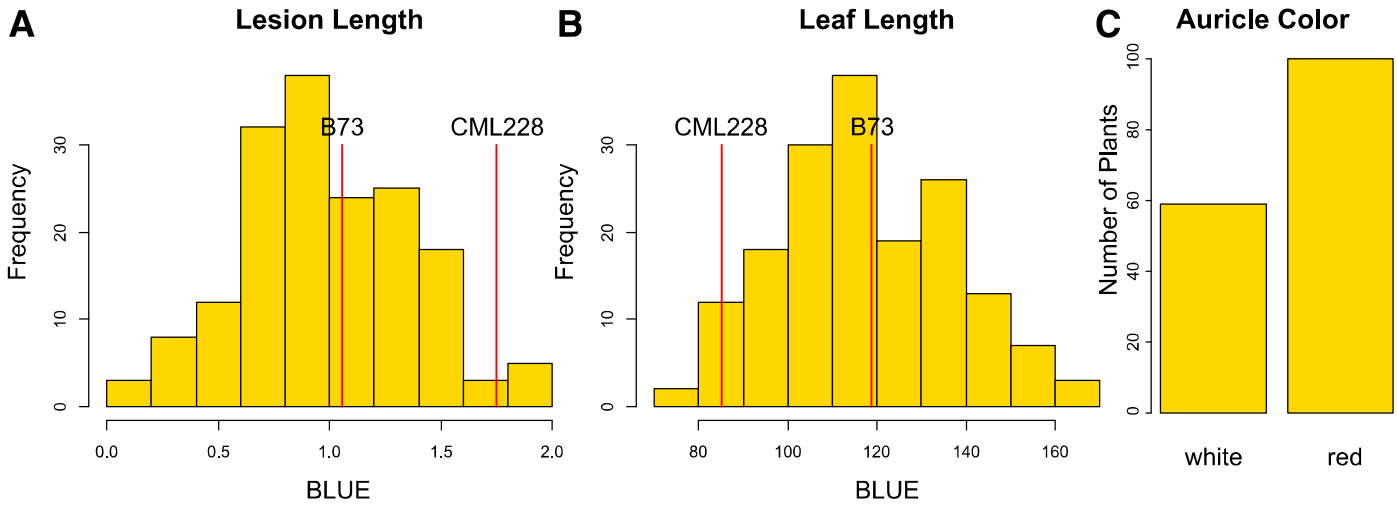

Fig. 2. Phenotypic distributions of best linear unbiased estimates (BLUEs). **A,** Lesion length; **B,** leaf length; and **C,** auricle color.

TABLE 2. Analysis of variance table of the lesion length model and associated *P* values

Factor	Degrees of freedom	Sum of squares	Mean of squares	F value	*P* (>F)
Genotype	167	96.77	0.5795	4.080	<2e-16
Rep	2	0.38	0.1918	1.351	0.260366
Rep:block	15	6.09	0.4062	2.860	0.000287
Residuals	372	52.84	0.1420		

(Qiu et al. 2020a). To test whether there was a relationship between BLS resistance and resistance to other pathogens, we examined the correlations among BLS and three common fungal diseases. Lesion length had a weak negative correlation with southern corn leaf blight ($P = 0.087$, r = −0.13), indicating that lines resistant to BLS tend to be susceptible to southern corn leaf blight, and a weak positive correlation with gray leaf spot (GLS; $P = 0.072$, r = 0.16), indicating that lines resistant to BLS tended to be resistant to GLS as well. Although several of these correlations are significant, many were very weak, indicating that these traits are largely independent of BLS resistance.

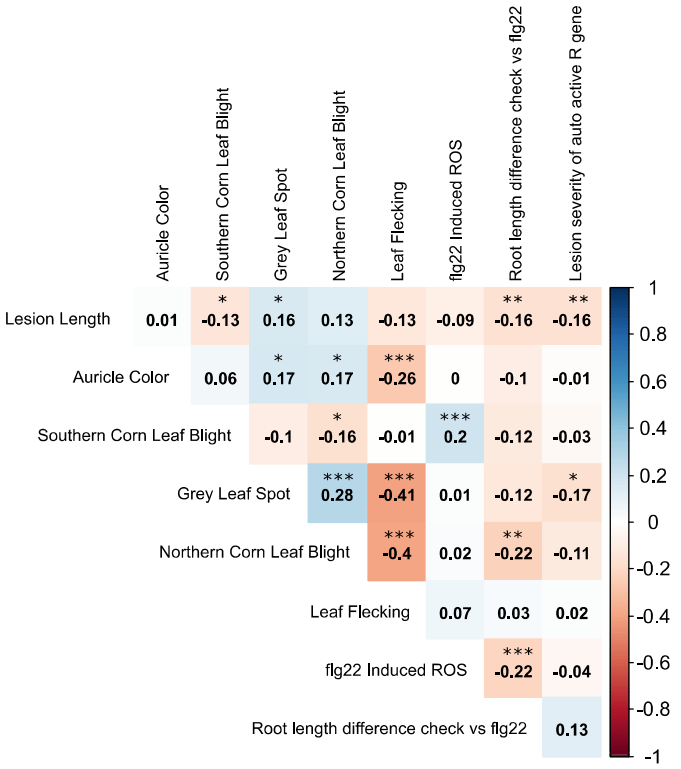

Fig. 4. Correlation plot of the phenotypic data that have been collected for this population. The values inside the boxes are the Pearson correlation coefficients for all trait combinations except auricle color, which is a biserial correlation coefficient. Significance values symbols indicate the following: * at alpha = 0.1; ** at alpha = 0.05; *** at alpha = 0.01. Blue represents positive correlations. Red represents negative correlations. The trait difference in root length is the difference in root length between check and flg22-treated seedlings (Wang et al. 2021). Higher values indicate more growth inhibition due to flg22 treatment and thus a stronger pattern-triggered immunity response. The trait lesion severity of an autoactive R gene was rated on a 1 to 10 scale, with 10 being the most severe, indicating a strong hypersensitive response (Olukolu et al. 2014).

While conducting the disease screening trials, we noticed that there was variation within the population for auricle color (red or white). Red coloration of plant organs in maize is often due to the accumulation of phlobaphene and, in some cases, anthocyanins (Cassani et al. 2016; Grotewold et al. 1994; Mol et al. 1998; Ryu et al. 2013). Previous studies have demonstrated a relationship between phlobaphenes in the pericarp and fumonisin accumulation (Landoni et al. 2020). We hypothesized that plants that had red auricles and accumulated more pigment might be more resistant to some diseases. Although we found no relationship between auricle color and BLS severity, there was a relationship between auricle color, GLS, northern corn leaf blight, and leaf flecking (Fig. 4). Interestingly, the strongest relationship was with leaf flecking, where lines with red auricles tended to have less flecking ($P = 6.5e\text{-}04$, r = −0.26). Spontaneous spots of leaf necrosis, or flecking, have been previously observed to be segregating in this population (Olukolu et al. 2016), We reanalyzed the Olukolu et al. (2016) data using our marker dataset and identified a leaf flecking QTL on chromosome 6 that colocalized with the auricle color QTL (Table 3).

Discussion

We examined relationships among BLS resistance and other disease- and defense-related traits in an RIL mapping population derived from a B73 × CML228 cross. We mapped QTLs for BLS resistance and found significant but weak relationships between BLS resistance, PTI, and hypersensitive response phenotypes. Little is known about the genetic architecture of resistance to BLS (Qiu et al. 2020b), and this study provides additional insights into the genetics of resistance that can be useful in a breeding context.

Previous studies found a weak correlation between BLS and northern corn leaf blight (Qiu et al. 2020a, b). This is consistent with the weak correlation we found in this study between BLS and GLS. None of the QTLs we identified for BLS overlapped with previously identified BLS QTLs (Qiu et al. 2020b). Few populations have been evaluated at this point for BLS resistance; thus, there are many novel resistance loci that are yet to be discovered.

We had previously assessed levels of PTI response by measuring ROS production in response to flg22 using the same population as Zhang et al. (2017). Because *X. vasicola* pv. *vasculorum* has a flagellum, we hypothesized that PTI, as assessed by measuring the plant response to flg22, might be related to BLS resistance, but the evidence to support this hypothesis was weak. The weak

TABLE 3. Linkage mapping results, with phenotypic data for field leaf flecking from Olukolu et al. (2016) and flg22 reactive oxygen species (ROS) from Zhang et al. (2017)

Phenotype	Chr[a]	Bin[b]	Physical position[c]	Peak marker	LOD[d]	A[e]	R^2 (%)[f]	Bayes interval[g]
Lesion length	2	2.07	196,469,668	m1595	3.742	0.1055	8.175	192,506,605–210,154,296
Lesion length	5	5.03	19,788,296	m3703	4.655	0.1194	10.304	14,579,312–150,355,506
Lesion length	7	7.00	5,957,665	m4917	3.852	−0.1078	8.43	3,058,132–109,153,734
Auricle color	6	6.05	124,311,357	m4461	4.5	0.764	12.3	109,282,082–148,860,589
Leaf length	4	4.08	185,120,016	m3187	4.4	−6.6	11.6	157,449,995–206,850,914
Leaf flecking	6	6.05	144,566,010	m4514	9.77	−0.2225	22.25	135,282,882–146,170,131
flg22 ROS	2	2.06	175,104,072	m1495	5.6	−151.6	13.85	167,417,879–183,990,538

[a] Chromosome.
[b] Bin, chromosome bin location for significant quantitative trait locus (Davis et al. 1999).
[c] Physical position of peak marker in base pairs (bp) (RefGen_v3).
[d] LOD, logarithm of odds value at the position of the peak likelihood of the quantitative trait locus (QTL).
[e] A, additive effect estimates of the detected QTL. Effects are in terms of the disease rating scale used. The positive value indicates that the CML228 allele increases resistance in the first two QTLs for lesion length; for leaf length, the negative value indicates the B73 allele decreases leaf length; auricle color's positive value indicates that the B73 allele is associated with darker colored auricles; the CML228 allele increases Flg22 ROS; the CML228 allele increases flecking.
[f] Percentage of phenotypic variance explained by the detected QTL.
[g] The interval in base pairs for which the LOD values are significant.

correlation and lack of overlapping QTLs might be due to multiple factors. It is important to note that we only measured one aspect of PTI. Other measures of PTI might have higher correlations with BLS resistance. Another possibility is that PTI is not the only line of defense that plants employ to protect from pathogen invasion and colonization, and resistance is often due to factors other than PTI. Part of the reason plants cannot rely entirely on PTI is because bacteria secrete effectors that supplant PTI, and *X. vasicola* pv. *vasculorum* has effectors that are predicted to be suppressors of PTI (Perez-Quintero et al. 2020).

A potential reason the correlations were not stronger could be due to the flg22 epitope, or version of flg22, used in PTI assays being different from the one present in *X. vasicola* pv. *vasculorum* (Wang et al. 2021). The epitope used for the PTI studies is from *Pseudomonas aeruginosa* (Wang et al. 2021; Zhang et al. 2017). The flg22 epitope from *X. vasicola* pv. *vasculorum* only has 77.2% amino acid sequence identity with the synthetic flg22 epitope used in the maize PTI assays (Clarke et al. 2013; Stulberg et al. 2020; Wang et al. 2021; Zhang et al. 2017). Plants have differential ROS responses to different epitopes of flg22 from different strains of the same bacterial species (Clarke et al. 2013). Many commensal and endophytic bacteria have been shown to possess flg22 epitopes capable of evading the immune responses of their hosts (Colaianni et al. 2021; Trdá et al. 2014). Thus, using a different epitope for PTI assays might lead to stronger correlations with BLS resistance and the detection of common genetic regions for BLS resistance and PTI responses.

Similar weak correlations between flg22-induced PTI and disease severity have been observed in other pathosystems (Bhattarai et al. 2016). Diverse tomato lines were assayed for ROS production in response to different epitopes of flg22 derived from *Pseudomonas* and *Xanthomonas* species. The lines were then evaluated for their resistance to *Xanthomonas perforans.* There was no correlation between disease severity and ROS-induced response to the *Pseudomonas* epitopes of flg22, but there was a weak correlation between the ROS induced by the *Xanthomonas* epitope of flg22 and disease severity (Bhattarai et al. 2016). Taken together, these observations indicate that flg22 immune responses vary quantitatively due to allelic diversity of flagellin epitopes and variation in the plant's ability to perceive any particular epitope of flagellin.

Flavonoids are widely known to be involved in plant-pathogen interactions (Koes et al. 1994), and pigmented flavonoids, such as anthocyanins and phlobophenes, are deposited in various plant organs in maize, including the auricles. We examined whether there was a relationship between auricle color and disease severity. Although no strong relationships were identified between disease severity and auricle color, we did find that plants with red auricles tended to have less flecking than those with white auricles. The chromosome 6 auricle color QTL overlaps with the chromosome 6 QTL for leaf flecking (Table 3). We only collected one replication of data for auricle color; auricle color is known to be involved with phlobophene and anthocyanin accumulation. Red auricles are distinct from purple auricles and may be related to salmon silks based on observations of segregating populations derived from salmon silk mutants (Andorf et al. 2015). Populations segregating for *Salmon silks* mutations segregate for auricle and silk color, and *salmon silks1* (*sm1*) is located within the confidence interval for the auricle color QTL we identified (Casas et al. 2016). *Sm1* encodes a multidomain UDP-rhamnose synthase and is part of the biosynthetic pathway of maysin, an important insecticidal flavone produced by maize (Casas et al. 2016). Chromosomal bin 6.05 has been identified in other studies as conferring resistance to multiple diseases. QTLs for northern corn leaf blight and anthracnose stalk rot resistance identified in other populations colocalize with the auricle color and leaf flecking QTLs identified in this study (Chung et al. 2011; Morales et al. 2020; Poland et al. 2011). Further work is needed to explore the relationship between auricle color, pigmented flavonoids and defense in maize.

In conclusion, we have identified novel QTLs for BLS resistance in maize that will contribute to the limited knowledge available regarding the genetic architecture of resistance to BLS. In addition, we observed significant, but weak, correlations between BLS severity and some PTI traits. This work was a first step in examining the relationship between BLS resistance and PTI. Further work is needed to understand what mechanisms underlie BLS resistance.

Literature Cited

Andorf, C. M., Cannon, E. K., Portwood, J. L., II, Gardiner, J. M., Harper, L. C., Schaeffer, M. L., Braun, B. L., Campbell, D. A., Vinnakota, A. G., Sribalusu, V. V., Huerta, M., Cho, K. T., Wimalanathan, K., Richter, J. D., Mauch, E. D., Rao, B. S., Birkett, S. M., Sen, T. Z., and Lawrence-Dill, C. J. 2015. MaizeGDB update: New tools, data and interface for the maize model organism database. Nucleic Acids Res. 44:D1195-D1201.

Balint-Kurti, P. 2019. The plant hypersensitive response: Concepts, control and consequences. Mol. Plant Pathol. 20:1163-1178.

Barak, J. D., Koike, S. T., and Gilbertson, R. L. 2001. Role of crop debris and weeds in the epidemiology of bacterial leaf spot of lettuce in California. Plant Dis. 85:169-178.

Bates, D., Mächler, M., Bolker, B., and Walker, S. 2015. Fitting linear mixed-effects models using lme4. J. Stat. Softw. 67:1-48.

Benson, J. M., Poland, J. A., Benson, B. M., Stromberg, E. L., and Nelson, R. J. 2015. Resistance to gray leaf spot of maize: Genetic architecture and mechanisms elucidated through nested association mapping and near-isogenic line analysis. PLoS Genet. 11:e1005045.

Bhattarai, K., Louws, F. J., Williamson, J. D., and Panthee, D. R. 2016. Differential response of tomato genotypes to *Xanthomonas*-specific pathogen-associated molecular patterns and correlation with bacterial spot (*Xanthomonas perforans*) resistance. Hortic. Res.-England 3.

Boller, T., and Felix, G. 2009. A renaissance of elicitors: Perception of microbe-associated molecular patterns and danger signals by pattern-recognition receptors. Annu. Rev. Plant Biol. 60:379-406.

Broman, K. W., Wu, H., Sen, Ś., and Churchill, G. A. 2003. R/qtl: QTL mapping in experimental crosses. Bioinformatics 19:889-890.

Casas, M. I., Falcone-Ferreyra, M. L., Jiang, N., Mejía-Guerra, M. K., Rodríguez, E., Wilson, T., Engelmeier, J., Casati, P., and Grotewold, E. 2016. Identification and characterization of maize salmon silks genes involved in insecticidal maysin biosynthesis. Plant Cell 28:1297-1309.

Cassani, E., Puglisi, D., Cantaluppi, E., Landoni, M., Giupponi, L., Giorgi, A., and Pilu, R. 2016. Genetic studies regarding the control of seed pigmentation of an ancient European pointed maize *(Zea mays* L.) rich in phlobaphenes: The "Nero Spinoso" from the Camonica valley. Genet. Resour. Crop Evol. 64:761-773.

Chung, C. L., Poland, J., Kump, K., Benson, J., Longfellow, J., Walsh, E., Balint-Kurti, P., and Nelson, R. 2011. Targeted discovery of quantitative trait loci for resistance to northern leaf blight and other diseases of maize. Theor. Appl. Genet. 123:307-326.

Clarke, C. R., Chinchilla, D., Hind, S. R., Taguchi, F., Miki, R., Ichinose, Y., Martin, G. B., Leman, S., Felix, G., and Vinatzer, B. A. 2013. Allelic variation in two distinct *Pseudomonas syringae* flagellin epitopes modulates the strength of plant immune responses but not bacterial motility. New Phytol. 200:847-860.

Colaianni, N. R., Parys, K., Lee, H.-S., Conway, J. M., Kim, N. H., Edelbacher, N., Mucyn, T. S., Madalinski, M., Law, T. F., and Jones, C. D. 2021. A complex immune response to flagellin epitope variation in commensal communities. Cell Host Microbe 29:635-649. e639.

Coll, N. S., Epple, P., and Dangl, J. L. 2011. Programmed cell death in the plant immune system. Cell Death Differ. 18:1247-1256.

Coutinho, T. A., and Wallis, F. M. 1991. Bacterial streak disease of maize (*Zea mays* L.) in South Africa. J. Phytopathol. 133:112-112.

Damicone, J., Cevallos, F., and Olson, J. 2018. First report of bacterial leaf streak of corn caused by *Xanthomonas vasicola* pv. *vasculorum* in Oklahoma. Plant Dis. 102:437-437.

Davis, G. L., McMullen, M. D., Baysdorfer, C., Musket, T., Grant, D., Staebell, M., Xu, G., Polacco, M., Koster, L., Melia-Hancock, S., Houchins, K., Chao, S., and Coe, E. H. 1999. A maize map standard with sequenced core markers, grass genome reference points and 932 expressed sequence tagged sites (ESTs) in a 1736-locus map. Genetics 152:1137-1172.

Duin, I. M., Forasteiro, T. A., Rodrigues, V. H. S., Balbi-Peña, M. I., and Júnior, R. P. L. 2022. In vitro sensitivity of *Xanthomonas vasicola* pv. *vasculorum* and the control of bacterial leaf streak of corn with copper oxychloride alone and in mixtures with mancozeb and fluxapyroxad. Eur. J. Plant Pathol. 164:263-268.

Dyer, R. A. 1949. Botanical surveys and control of plant diseases. Farming in South Africa 24.

Freeling, M., and Lane, B. 1994. The maize leaf. Pages 17-28 in: The Maize Handbook. M. Freeling and V. Walbot, eds. Springer, New York.

Gent, D. H., Lang, J. M., Bartolo, M. E., and Schwartz, H. F. 2005. Inoculum sources and survival of *Xanthomonas axonopodis* pv. *allii* in Colorado. Plant Dis. 89:507-514.

Grotewold, E., Drummond, B. J., Bowen, B., and Peterson, T. 1994. The Myb-homologous P-gene controls phlobaphene pigmentation in maize floral organs by directly activating a flavonoid biosynthetic gene subset. Cell 76: 543-553.

Hartman, T., Harbour, J., Tharnish, B., Van Meter, J., and Jackson-Ziems, T. A. 2020b. Agronomic factors associated with bacterial leaf streak development caused by *Xanthomonas vasicola* pv. *vasculorum* in corn. Phytopathology 110:1132-1138.

Hartman, T., Tharnish, B., Harbour, J., Yuen, G. Y., and Jackson-Ziems, T. A. 2020a. Alternative hosts in the families *Poaceae* and *Cyperaceae* for *Xanthomonas vasicola* pv. *vasculorum*, causal agent of bacterial leaf streak of corn. Phytopathology 110:1147-1152.

Jamann, T. M., Plewa, D., Mideros, S. X., and Bissonnette, S. 2019. First report of bacterial leaf streak of corn caused by *Xanthomonas vasicola* pv. *vasculorum* in Illinois. Plant Dis. 103:1018-1018.

Jones, J. D. G., and Dangl, J. L. 2006. The plant immune system. Nature 444: 323-329.

Kimball, J., Cui, Y., Chen, D., Brown, P., Rooney, W. L., Stacey, G., and Balint-Kurti, P. J. 2019. Identification of QTL for target leaf spot resistance in sorghum bicolor and investigation of relationships between disease resistance and variation in the MAMP response. Sci. Rep. 9:18285.

Koes, R. E., Quattrocchio, F., and Mol, J. N. M. 1994. The flavonoid biosynthetic-pathway in plants - Function and evolution. BioEssays 16:123-132.

Korus, K., Lang, J. M., Adesemoye, A. O., Block, C. C., Pal, N., Leach, J. E., and Jackson-Ziems, T. A. 2017. First report of *Xanthomonas vasicola* causing bacterial leaf streak on corn in the United States. Plant Dis. 101: 1030-1031.

Kump, K. L., Bradbury, P. J., Wisser, R. J., Buckler, E. S., Belcher, A. R., Oropeza-Rosas, M. A., Zwonitzer, J. C., Kresovich, S., McMullen, M. D., Ware, D., Balint-Kurti, P. J., and Holland, J. B. 2011. Genome-wide association study of quantitative resistance to southern leaf blight in the maize nested association mapping population. Nat. Genet. 43:163-168.

Landoni, M., Puglisi, D., Cassani, E., Borlini, G., Brunoldi, G., Comaschi, C., and Pilu, R. 2020. Phlobaphenes modify pericarp thickness in maize and accumulation of the fumonisin mycotoxins. Sci. Rep.-UK 10.

Lang, J. M., DuCharme, E., Ibarra Caballero, J., Luna, E., Hartman, T., Ortiz-Castro, M., Korus, K., Rascoe, J., Jackson-Ziems, T. A., Broders, K., and Leach, J. E. 2017. Detection and characterization of *Xanthomonas vasicola* pv. *vasculorum* (Cobb 1894) comb. nov. causing bacterial leaf streak of corn in the United States. Phytopathology 107:1312-1321.

Leite, R. P., Custodio, A. A. P., Madalosso, T., Robaina, R. R., Duin, I. M., and Sugahara, V. H. 2019. First report of the occurrence of bacterial leaf streak of corn caused by *Xanthomonas vasicola* pv. *vasculorum* in Brazil. Plant Dis. 103:145-145.

Lloyd, S. R. 2014. Mapping PAMP Responses and Disease Resistance in Brassicas. University of East Anglia.

Lloyd, S. R., Schoonbeek, H. J., Trick, M., Zipfel, C., and Ridout, C. J. 2014. Methods to study PAMP-triggered immunity in *Brassica* species. Mol. Plant-Microbe Interact. 27:286-295.

Longhi, T. V., Robaina, R. R., Júnior, R. P. L., and Balbi-Peña, M. I. 2022. Sensibility of *Xanthomonas vasicola* pv. *vasculorum* to chemicals and efficiency of the chemical control of bacterial leaf streak on corn plants. Acta Scientiarum 44.

Mol, J., Grotewold, E., and Koes, R. 1998. How genes paint flowers and seeds. Trends Plant Sci. 3:212-217.

Morales, L., Repka, A., Swarts, K. L., Stafstrom, W. C., He, Y., Sermons, S. M., Yang, Q., Lopez-Zuniga, L. O., Rucker, E., and Thomason, W. E. 2020. Genotypic and phenotypic characterization of a large, diverse population of maize near-isogenic lines. Plant J. 103:1246-1255.

Ogut, F., Bian, Y., Bradbury, P. J., and Holland, J. B. 2015. Joint-multiple family linkage analysis predicts within-family variation better than single-family analysis of the maize nested association mapping population. Heredity 114:552-563.

Olukolu, B. A., Bian, Y., De Vries, B., Tracy, W. F., Wisser, R. J., Holland, J. B., and Balint-Kurti, P. J. 2016. The genetics of leaf flecking in maize and its relationship to plant defense and disease resistance. Plant Physiol. 172:1787-1803.

Olukolu, B. A., Wang, G. F., Vontimitta, V., Venkata, B. P., Marla, S., Ji, J., Gachomo, E., Chu, K., Negeri, A., Benson, J., Nelson, R., Bradbury, P., Nielsen, D., Holland, J. B., Balint-Kurti, P. J., and Johal, G. 2014. A genome-wide association study of the maize hypersensitive defense response identifies genes that cluster in related pathways. PLoS Genet. 10:e1004562.

Ortiz-Castro, M. 2019. Understanding the disease ecology of the corn bacterial leaf streak pathogen *Xanthomonas vasicola* pv. *vasculorum*. Dissertation. Colorado State University, Fort Collins, CO.

Ortiz-Castro, M., Hartman, T., Coutinho, T., Lang, J. M., Korus, K., Leach, J. E., Jackson-Ziems, T., and Broders, K. 2020. Current understanding of the history, global spread, ecology, evolution, and management of the corn bacterial leaf streak pathogen, *Xanthomonas vasicola* pv. *vasculorum*. Phytopathology 110:1124-1131.

Perez-Quintero, A. L., Ortiz-Castro, M., Lang, J. M., Rieux, A., Wu, G., Liu, S., Chapman, T. A., Chang, C., Ziegle, J., Peng, Z., White, F. F., Plazas, M. C., Leach, J. E., and Broders, K. 2020. Genomic acquisitions in emerging populations of *Xanthomonas vasicola* pv. *vasculorum* infecting corn in the United States and Argentina. Phytopathology 110:1161-1173.

Plazas, M. C., De Rossi, R. L., Brucher, L., Guerra, F. A., Vilaro, M., Guerra, G. D., Wu, G., Ortiz-Castro, M. C., and Broders, K. 2018. First report of *Xanthomonas vasicola* pv. *vasculorum* causing bacteria leaf streak of maize (*Zea mays*) in Argentina. Plant Dis. 102:1026-1026.

Poland, J. A., Bradbury, P. J., Buckler, E. S., and Nelson, R. J. 2011. Genome-wide nested association mapping of quantitative resistance to northern leaf blight in maize. Proc. Natl. Acad. Sci. U.S.A. 108.

Qiu, Y., Cooper, J., Kaiser, C., Wisser, R., Mideros, S. X., and Jamann, T. M. 2020a. Identification of loci that confer resistance to bacterial and fungal diseases of maize. G3 (Bethesda) 10:2819-2828.

Qiu, Y., Kaiser, C., Schmidt, C., Broders, K., Robertson, A. E., and Jamann, T. M. 2020b. Identification of quantitative trait loci associated with maize resistance to bacterial leaf streak. Crop Sci. 60:226-237.

R Core Team. 2021. R: A Language and Environment for Statistical Computing. R Foundation for Statistical Computing.

Robaina, R. R., Longhi, T. V., Zcffa, D. M., Gon alvcs, L. S. A., and Lcitc, R. P. 2020. Development of a protocol and a diagrammatic scale for quantification of bacterial leaf streak disease on young plants of maize. Plant Dis. 104: 2921-2927.

Ryu, S. H., Werth, L., Nelson, S., Scheerens, J. C., and Pratt, R. C. 2013. Variation of kernel anthocyanin and carotenoid pigment content in USA/Mexico borderland land races of maize. Econ. Bot. 67:98-109.

Samira, R., Kimball, J. A., Samayoa, L. F., Holland, J. B., Jamann, T. M., Brown, P. J., Stacey, G., and Balint-Kurti, P. J. 2020. Genome-wide association analysis of the strength of the MAMP-elicited defense response and resistance to target leaf spot in sorghum. Sci. Rep. 10:20817.

Schaad, N. W., Wang, Z. K., Di, M., McBeath, J., Peterson, G. L., and Bonde, M. R. 1996. An improved infiltration technique to test the pathogenicity of *Xanthomonas oryzae* pv *oryzae* in rice seedlings. Seed Sci. Technol. 24: 449-456.

Stulberg, M. J., Santillana, G., Studholme, D. J., Kasiborski, B., Ortiz-Castro, M., Broders, K., Arias, S., Block, C., Munkvold, G., and Rascoe, J. 2020. Genomics-informed molecular detection of *Xanthomonas vasicola* pv. *vasculorum* strains causing severe bacterial leaf streak of corn. Phytopathology 110:1174-1179.

Trdá, L., Fernandez, O., Boutrot, F., Héloir, M. C., Kelloniemi, J., Daire, X., Adrian, M., Clément, C., Zipfel, C., and Dorey, S. 2014. The grapevine flagellin receptor Vv FLS 2 differentially recognizes flagellin-derived epitopes from the endophytic growth-promoting bacterium *Burkholderia phytofirmans* and plant pathogenic bacteria. New Phytol. 201:1371-1384.

Venables, W. N., and Ripley, B. D. 2002. Modern Applied Statistics with S, 4th ed. Springer, New York.

Vetter, M. M., Kronholm, I., He, F., Haweker, H., Reymond, M., Bergelson, J., Robatzek, S., and de Meaux, J. 2012. Flagellin perception varies quantitatively in *Arabidopsis thaliana* and its relatives. Mol. Biol. Evol. 29: 1655-1667.

Wang, Y., Holland, J., and Balint-Kurti, P. 2021. Development and use of a seedling growth retardation assay to quantify and map loci underlying variation in the maize basal defense response. PhytoFrontiers 1:149-159.

Wei, T., Simko, V., Levy, M., Xie, Y., Jin, Y., and Zemla, J. 2017. Package 'corrplot'. Statistician 56:e24.

Wiesner-Hanks, T., and Nelson, R. 2016. Multiple disease resistance in plants. Annu. Rev. Phytopathol. 54:229-252.

Zhang, X., Valdes-Lopez, O., Arellano, C., Stacey, G., and Balint-Kurti, P. 2017. Genetic dissection of the maize (*Zea mays* L.) MAMP response. Theor. Appl. Genet. 130:1155-1168.